The Yellow Polymorphs of Mercuric Iodide (HgI_2)

by **Marc Hostettler**[1]), **Henrik Birkedal**[2]), and **Dieter Schwarzenbach***

Institute of Crystallography, University of Lausanne, CH-1015 Lausanne
(phone: ++4121 6923772; fax: ++4121 6923745; e-mail: dieter.schwarzenbach@ic.unil.ch)

Dedicated to Professor *Jack D. Dunitz* on the occasion of his 80th birthday

HgI_2 crystallizes under ambient conditions from various solvents and by sublimation into three concomitant polymorphs whose colors are red, orange, and yellow. The orange and yellow phases are metastable and transform into the red phase when touched. A phase transition from red to yellow occurs at 400 K. The reverse transition from yellow to red shows a huge hysteresis. We established that the structures of the metastable yellow^{M} phase (determined by single-crystal X-ray diffraction) and the high-temperature yellow^{HT} phase (determined by powder synchrotron X-ray diffraction and second-harmonic generation) are different, albeit closely related. Both show analogous packings of I–Hg–I molecules, which are straight in the first and bent with an angle of *ca.* 160° in the second. The red and orange phases are tetrahedral semiconductor structures that sublime even at room temperature. The growth of the yellow^{M} phase from 2-chloroethanol and the kinetics of the reconstructive phase transition red to yellow^{HT} and back were studied by optical microscopy, *Raman* spectroscopy in solution, luminescence, and powder synchrotron X-ray diffraction as a function of time at various temperatures. Both yellow phases grow by accretion of HgI_2 molecules, present in the solution or liberated from the red crystals, on the surface of the crystal. In contrast, the reverse transformation from yellow to red occurs in the bulk of the crystal, presumably by migration of Hg in the packing of I and subsequent rearrangement of I. The displacement parameters of Hg in both structures are considerably larger than those of I and apparently not dominated by disorder effects.

Introduction. – Mercuric iodide (HgI_2) is known to crystallize both from solution and by sublimation in three concomitant polymorphs: red, orange, and yellow crystals grow in the same batch [1]. The red phase is stable under ambient conditions. It has been intensively studied since the discovery of its opto-electronic properties [2], and its crystals are currently used as components in γ- and X-ray detectors [3][4]. The structure is tetragonal, space-group symmetry $P4_2/nmc$. The I-atoms form a cubic closest packing (ccp) of spheres, and the Hg-atoms occupy tetrahedral voids such as to form layers of corner-shared HgI_4 tetrahedra where all I–Hg–I and Hg–I–Hg angles are tetrahedral [5]. The orange phase comprises three different tetragonal crystal structures, which differ from the red phase only by the distribution of Hg in the ccp arrangement of I, all angles again being tetrahedral. All three orange structures feature corner-linked Hg_4I_{10} supertetrahedra. Two of them are end members with the maximum degree of order of a polytypic family of layer structures, space-group symmetries $I4_1/amd$ and $P4_2/nmc$ [6]. The third shows a three-dimensional linkage with symmetry $I4_1/acd$ [7]. In contrast, the structure of the yellow polymorph, as reported

[1]) Present address: Laboratorium für Kristallographie, Universität Bern, Freiestrasse 3, CH-3012 Bern.
[2]) Present address: Department of Chemistry and Biochemistry, University of California, Santa Barbara, CA 93106 – 9510, USA.

for a single crystal obtained by sublimation [5], is very different: it is molecular showing almost linear (178.3°) I–Hg–I molecules. Its symmetry is orthorhombic $Cmc2_1$. In the following, we refer to this phase as yellow^M. Both the orange and yellow^M crystals are mechanically unstable. When touched, red nuclei appear at the contact point and then grow throughout the sample. The mechanisms of these transformations are different for the two forms [8]. In the orange crystals, the red nuclei develop into irregularly shaped domains of slowly increasing volume. In contrast, in the much less stable yellow^M crystals, a red front propagates rapidly from the contact point and consumes the crystal [8].

At 400 K, the red form undergoes a destructive phase transition to a yellow form, yellow^{HT}, which has been assumed to be identical to the metastable yellow^M polymorph obtained under ambient conditions [9]. In addition, four additional phases of HgI_2 have been reported at moderate temperatures ($T < 700$ K) and pressures ($P < 4$ GPa) [9]. The general features of the phase diagram seem to be well known, but not all of its phases have been adequately characterized. Several of these high-pressure structures have been determined, at least qualitatively [10][11].

In this contribution, we present a study of the two yellow forms and the corresponding phase transitions of HgI_2. We report the crystallization of the red, orange, and yellow^M polymorphs by evaporation from a solution of 2-chloroethanol, *Raman* spectroscopy in solution, the crystal structures of the yellow^M and yellow^{HT} phases, and a study of the phase transition from red to yellow^{HT} at 400 K by powder diffraction.

Results and Discussion. – *Crystallization by Evaporation and* Raman *Spectroscopy in Solution.* The crystallization from a saturated solution of HgI_2 in 2-chloroethanol at room and elevated temperatures in open or closed vessels was investigated by optical microscopy. At room temperature in an open vessel, the three polymorphs crystallize consecutively: within the first few hours, only yellow nuclei become visible, after a day, the first orange crystals start to appear while the stable red crystals start to form after three days. A typical composition after complete evaporation of the solvent is shown in *Fig. 1,a*. The relative amounts of different types of crystal strongly depends on the temperature, with high temperature favoring the yellow polymorph. Above 323 K, this is the only product (*Fig. 1,b*). On the other hand, in a closed vessel at room temperature, only red, orange, and red/orange composite crystals are obtained (*Fig. 1,c*). Thus, rapid evaporation of the solvent is essential for the formation of yellow^M crystals, indicating that the crystallization of this form is governed by kinetics.

Raman spectra of the 2-chloroethanol solution show only two nonsolvent lines above 100 cm^{-1} with frequencies 139(4) and 159(2) cm^{-1} (*Fig. 2*). These are very similar to the frequencies of the Hg–I stretching mode observed for the yellow^{HT} phase (138 cm^{-1}) [12] and for the gaseous phase (158 cm^{-1}) [13], both of which feature molecular HgI_2 (see below and [14]). The mode at 114 cm^{-1} reported for the red phase [15] is not observed for the solution. This indicates that HgI_2 in solution exists in the form of molecules.

The observed crystallization sequence can now be understood as a kinetic effect. The molecules existing in solution rapidly pack into the yellow^M form while the formation of HgI_4 tetrahedra demands the breaking and creation of chemical bonds.

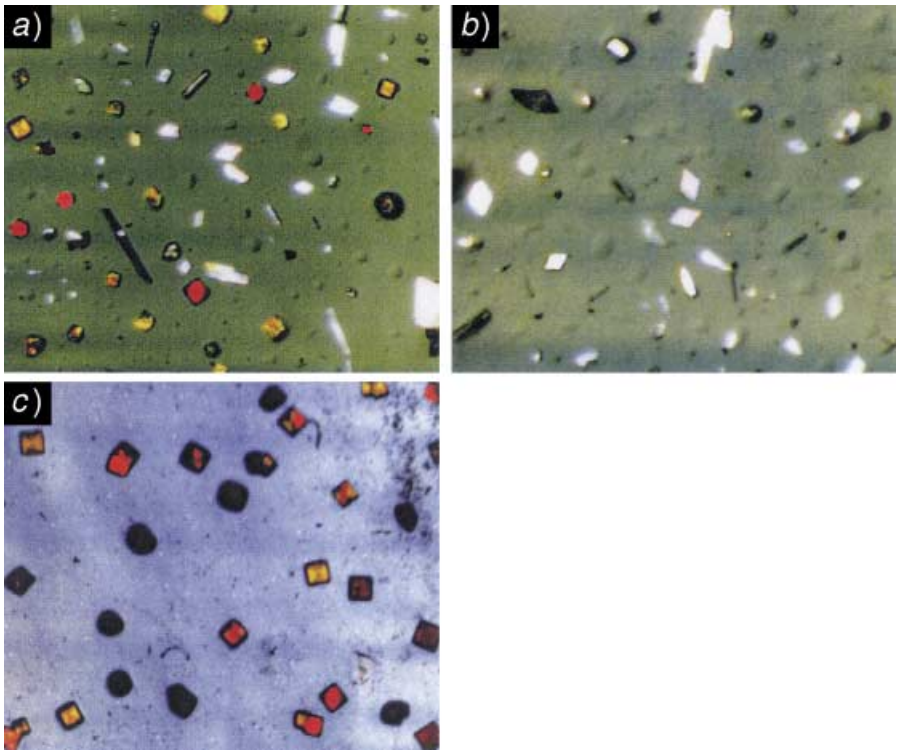

Fig. 1. a) *The three concomitant polymorphs of HgI_2 obtained by evaporation from a saturated solution of 2-chloroethanol at room temperature* (red, orange, and yellow^M crystals appear as dark-red, orange-yellow, and white, resp.) b) *Above 323 K, only the yellow^M form crystallizes.* c) *Leaving a saturated solution covered for six months at room temperature leads exclusively to red, orange, and red/orange composite crystals*

The least-stable yellow^M form is kinetically favored because HgI_2 is molecular in solution.

Second Harmonic Generation (SHG). The SHG signals of the red phase at 341 K and the yellow^{HT} phase at 410 K are shown in *Fig. 3*. The small maximum (just above the background level) generated by the red phase is attributed to the well-known surface effect. Since a surface amounts to a local symmetry breaking, the large number of crystallites contained in a powdered sample may generate a weak signal of SHG even for centrosymmetric materials. This weak signal remains unchanged up to 400(1) K, at which temperature the transformation to the yellow^{HT} phase occurs. A clear signal of SHG is then obtained from the high-temperature phase. This observation demonstrates the absence of an inversion center in the structure of the yellow^{HT} phase.

Luminescence. When excited with a 800-nm laser beam, the red phase generates a broad luminescence band at *ca.* 600 nm as illustrated in the inset of *Fig. 4*. In a study of the intensity of luminescence of the red phase as a function of purity, this band has been associated with the presence of impurities: right after synthesis, a strong signal was observed, while, after two cycles of purification by sublimation, the luminescence had disappeared [16].

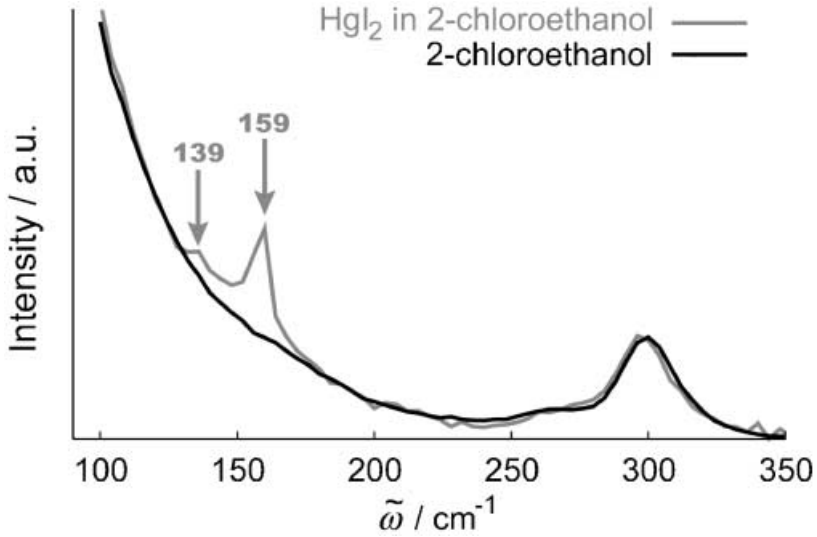

Fig. 2. Raman *spectrum of the solution of HgI_2 in 2-chloroethanol* (grey) *and of pure 2-chloroethanol* (black)

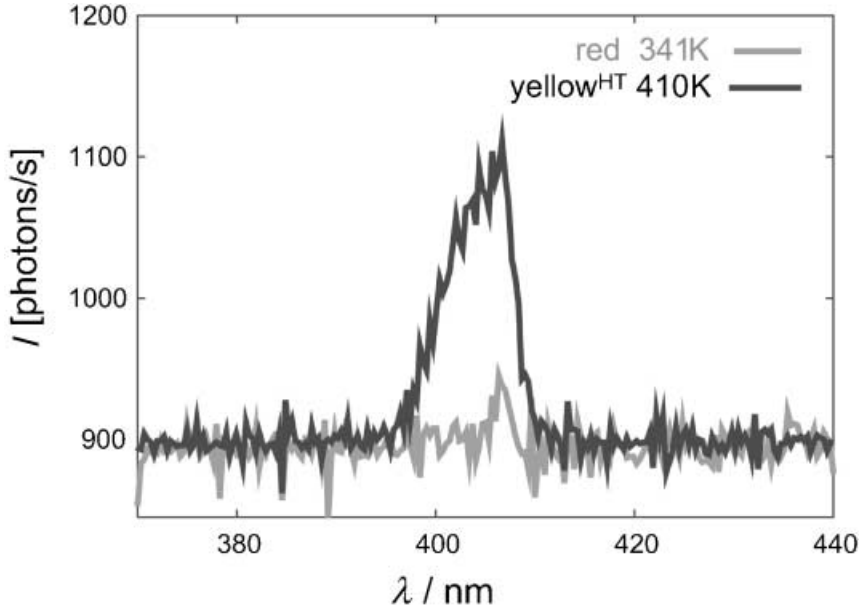

Fig. 3. *Second-harmonic signals generated by a 800-nm laser beam in the red phase* (grey), *and in the yellow high-temperature phase* (black)

With increasing temperature, we observe a progressive decrease of the intensity of luminescence up to the transition temperature red to yellow^{HT}, where the luminescence vanishes. The integrated intensity $I(T)$ of the luminescence band as a function of

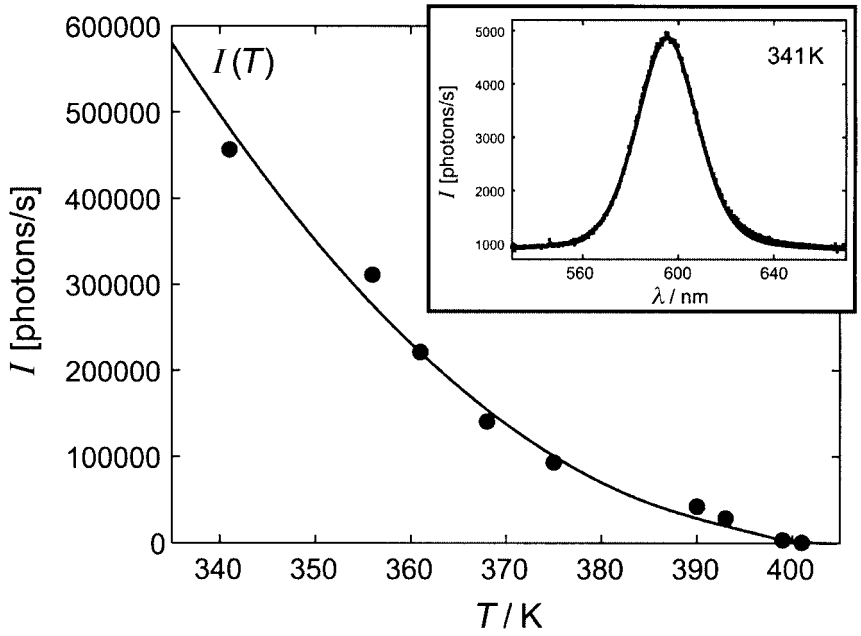

Fig. 4. *Integrated intensity of the luminescence* I *as a function of temperature* T. The inset shows the luminescence at T 341 K.

temperature allows to quantify this evolution. As illustrated in *Fig. 4*, a least-squares fit to a parabola gives $I(T) \approx 130(5) \cdot (T - T_c)^2$ where T_c 400 K is the transition temperature. When cooling the sample back to room temperature, the luminescence appears again, but now with a 50-times larger integrated intensity. This huge increase of luminescence may be explained by the formation of defects when the sample passes through the reconstructive yellow^{HT}-to-red-phase transition. In contrast, the decrease in intensity upon increasing temperature indicates that the defects, or the strains associated with defects, progressively disappear at higher temperatures, probably by diffusion and relaxation.

Crystal Structures. Single-crystal room-temperature X-ray data of a yellow^{M} crystal obtained by evaporation show the systematic absences of space group $Cmc2_1$ [5] (or *Cmcm*). The structure was solved by direct methods and subsequently refined by least-squares methods. The structural parameters are listed in *Table 1*. The results confirm the published structure derived with a crystal obtained by sublimation [5], but the parameters and, in particular, the thermal-displacement parameters are much more precise. The molecule is linear (*Fig. 5*): the I–Hg–I angle of 180.0(4)° is not imposed by symmetry. The atomic displacement parameters perpendicular to the chemical bond (U_{11} and U_{perp}) are larger than the one parallel to the axis of the dumbbell (U_{para}), as might be expected. The values of U_{para} of the three independent atoms are nearly identical suggesting rigid Hg–I bonds. In contrast, U_{11} and U_{perp} are considerably larger for the Hg atom than for the I-atoms. If the structure is ordered, the molecule is evidently not a rigid body.

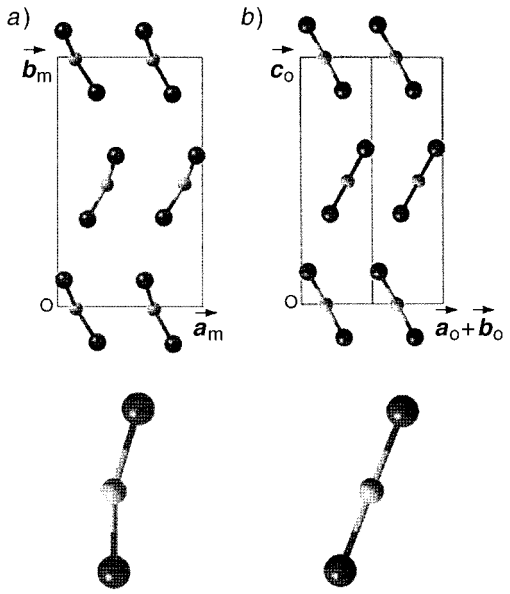

Fig. 5. *Structures* a) *of the yellow^{HT} phase, and* b) *of the yellow^{M} metastable polymorph*

Table 1. *Fractional Atomic Coordinates and Anisotropic Displacement Parameters in Å^2 of the Structure of the Yellow^{M} Metastable Polymorph at Room Temperature.* $U_{12}=U_{13}=0$ for all three atoms; U_{para} is along the molecular axis, U_{perp} is perpendicular to the axis in the mirror plane while U_{11} is normal to the mirror plane.

	x	y	z	U_{11}	U_{22}	U_{33}	U_{23}	U_{para}	U_{perp}
Hg	0.0	0.6586(5)	−0.0039(8)	0.093(2)	0.070(2)	0.094(2)	0.031(1)	0.051(3)	0.113(3)
I(1)	0.0	0.9106(6)	0.8632(3)	0.077(3)	0.054(2)	0.059(2)	0.006(2)	0.050(3)	0.063(3)
I(2)	0.0	0.4069(6)	0.1289(3)	0.076(3)	0.057(3)	0.054(2)	0.004(2)	0.052(3)	0.059(4)

The structure of the yellow^{HT} phase was studied by powder diffraction with synchrotron radiation and an area detector at T 412(2) K. The lattice constants, the systematic absences and the observation of a second-harmonic signal indicate the symmetry to be $P2_1$, a monoclinic subgroup of the space group $Cmc2_1$ of the room-temperature yellow^{M} structure. A model of the monoclinic structure was obtained by desymmetrizing the orthorhombic structure. A *Rietveld* refinement gave the fit presented in *Fig. 6*. A comparison of the two yellow structures is presented in *Fig. 5*. They are closely related, both showing I−Hg−I molecules. The asymmetric unit of the cell of the yellow^{HT} phase contains two independent molecules with similar geometries, the r.m.s. deviation between the respective atom positions being less than 0.08 Å. The principal difference between the yellow^{HT} and yellow^{M} structures is that the molecules are bent instead of linear and similar to those in the gas phase, with angles of 163(1)° for I(1)−Hg(1)−I(2), 157(1)° for I(3)−Hg(2)−I(4), and 170° in the gas phase as obtained by electron diffraction and by vibrational spectroscopy [14]. The angle between the molecular planes is 55.9°. The isotropic displacement parameters, one for Hg and one for I, are large (*Table 2*). Although the significance of displacement parameters obtained by *Rietveld* powder refinement may be doubtful because of

important correlations with parameters describing the background, it is noteworthy that the values for Hg are almost twice those for I. The displacement parameters of the metastable yellow^{M} structure perpendicular to the molecular axis show a similar effect. The intramolecular Hg–I distances are all comprised of intervals of 4 s.u. around the average value of 2.5 Å, which is 0.13 Å (4 s.u.) smaller than for the yellow^{M} polymorph or for the gas-phase structure [14]. It is well-known that structural disorder may result in apparently short distances. As HgI_2 sublimes already at room temperature and progressively more at higher temperatures, the structure of the yellow^{HT} phase may well be somewhat disordered.

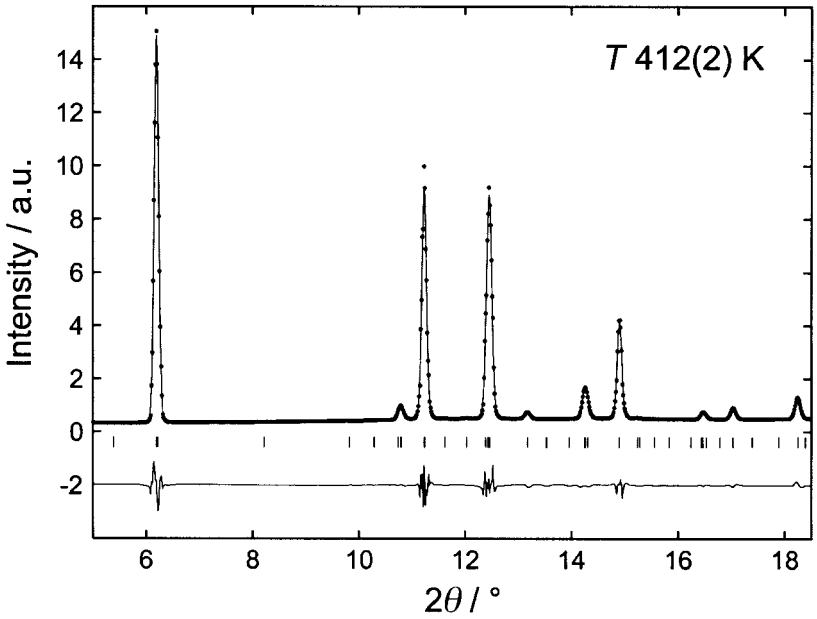

Fig. 6. *Low-angle region of the powder diagram of the yellow^{HT} phase.* Points show the observed, full line the calculated data, the difference is shifted to –2 for clarity.

Table 2. *Fractional Atomic Coordinates and Isotropic Displacement Parameters in Å^2 of the Structure of the Yellow^{HT} Phase at 412(2) K*

	x	*y*	*z*	U_{iso}
Hg(1)	0.160(3)	0.476(2)	0.497(4)	0.142(6)
Hg(2)	0.319(3)	–0.039(2)	–0.978(4)	0.142(6)
I(1)	0.028(3)	0.608(2)	0.142(4)	0.079(5)
I(2)	0.274(6)	0.387(2)	0.948(9)	0.079(5)
I(3)	0.233(3)	–0.144(2)	–0.394(4)	0.079(5)
I(4)	0.460(3)	0.171(2)	0.292(5)	0.079(5)

Kinetics of the Red-to-Yellow^{HT} Transition. The red-to-yellow^{HT} phase transition is first-order. According to earlier work [8], the mechanisms for the red → yellow^{HT} and the reverse yellow^{HT} → red transitions are different, and there exists a huge hysteresis. Upon heating, the transition occurs through surface nucleation while, upon cooling, it

shows bulk nucleation. The coexistence of the two phases over a large temperature range offers the possibility to study the kinetics of the transformation. Synchrotron powder-diffraction data collected in the coexistence region at different temperatures as a function of time provide information on the growth of one phase at the expense of the other.

The intensities of the powder-diffraction lines $(110)_r$ of the red phase and $(002)_y$ of the yellow^{HT} phase were used to follow the change of volume of the two phases with time. For the study of the red $\rightarrow$ yellow^{HT} transition at increasing temperatures, data were measured at the temperatures T_1 402.9(5) K and T_2 404.0(5) K. For small temperature differences, such as $T_2 - T_1$ of only 1 K, the structure factors do not vary significantly, and the integrated intensities of a reflection, thus, represent the amounts of the corresponding phase present in the sample. The integrated intensities of the $(002)_y$ reflection show that the growth of yellow^{HT} is faster at T_2 than at T_1 (*Fig. 7*). Thus, as expected, the speed of the transformation increases with temperature. The data points are well reproduced by quadratic polynomials. Compared to the linear coefficients, the quadratic contributions are negative and small and may be due to a decrease of material by sublimation of HgI_2. The linear coefficients, $k_1 = 3.6 \cdot 10^{-4} s^{-1}$ and $k_2 = 4.2 \cdot 10^{-4} s^{-1}$, are estimates of the growth rates of yellow^{HT}. From these rates, the activation energy of the transition can be calculated using *Arrhenius* law $k(T) = A \cdot \exp(-E_a/RT)$, where k is the growth rate in s^{-1}, A a frequency factor in s^{-1}, E_a the activation energy in $J \cdot mol^{-1}$, T the absolute temperature, and $R = 8.314\ J \cdot mol^{-1} \cdot K^{-1}$ the ideal gas constant [17]. For the red $\rightarrow$ yellow^{HT} transition, $A \approx 1.39 \cdot 10^{21} s^{-1}$ and $E_a \approx 190\ kJ \cdot mol^{-1}$.

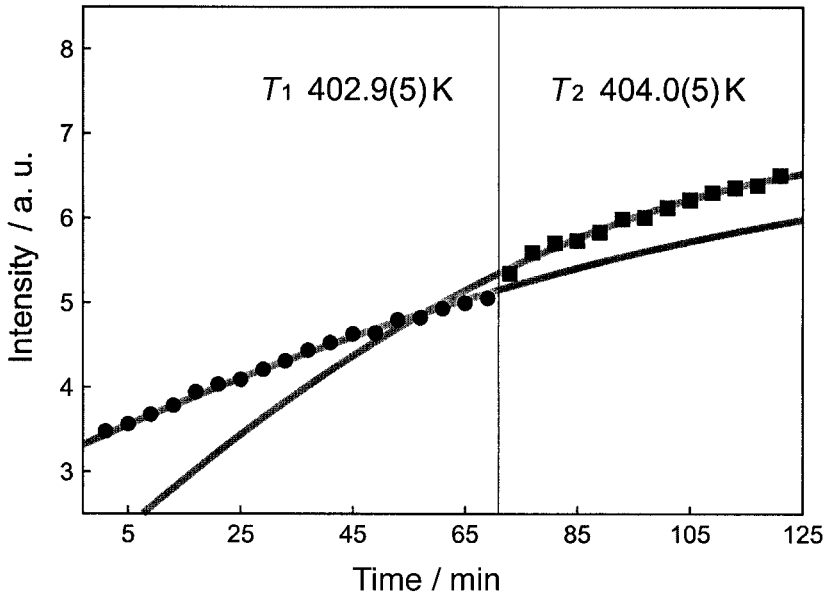

Fig. 7. *Kinetics of the red → yellow^{HT} transition*. The growth of the yellow^{HT} phase is monitored by the integrated intensity, normalized by the intensity of the primary beam, of the $(002)_y$ reflection as a function of time. Circles (●) for temperature T_1, squares (■) for T_2.

To study the kinetics of the reverse yellow^{HT} → red transition, data were collected as a function of time at the temperature T_3 381.3(5) K. There, the two phases coexist, and one observes the growth of the red phase at the expense of the yellow^{HT} one. The integrated intensities of $(110)_r$ and $(002)_y$ reveal linear volume changes of the two phases, as illustrated in *Fig. 8*. The transformation is much slower than in the red → yellow^{HT} direction. Whereas, in 1 h, 50% of the volume of the sample had transformed to yellow^{HT} at 403 K upon heating, only 10% transformed to red at 381 K upon cooling. The growth rate of the red phase at 381 K is $k_3 = 1.8 \cdot 10^{-5}\,s^{-1}$. It is worth mentioning that, at the end of the experiment at room temperature, the fraction of red crystals in the part of the sample hit by the X-ray beam was larger than in the rest of the sample. The observed value of k_3 is, thus, determined not only by the temperature but also by the flux of X-rays.

Thus, the kinetics of the red-to-yellow^{HT} transition are shown to be highly asymmetric. This agrees with the observation of two different nucleation mechanisms [8]. The hysteresis of the transition is also asymmetric in the sense that the yellow^{HT} phase may be cooled to room temperature while the red phase can be overheated to only *ca.* 10 K above the transition temperature. The quality of the data does not allow us to conclude that this cooled yellow^{HT} phase retains the high-temperature structure or is identical to the metastable phase grown at room temperature.

Conclusions. – In contrast to the traditional assumption of a single yellow molecular phase of HgI_2 at normal pressure, our study reveals the existence of two such phases, metastable yellow^{M} forming at room temperature by sublimation or crystallization from solution and high-temperature yellow^{HT} resulting from a phase transition at 400 K. Their structures are, however, closely related. Both space-group symmetries admit bent I–Hg–I molecules, but yellow^{M} shows straight molecules and yellow^{HT} two symmetrically independent bent molecules whose planes form an angle of close to 60°. The gas phase of HgI_2 also contains bent molecules [14]. At first glance, one is tempted to speculate that yellow^{M} is simply a disordered version of yellow^{HT} resulting from a superposition of bent molecules in different orientations, in agreement with the observation that the r.m.s. displacements of Hg perpendicular to the molecular axis are considerably larger than those of I. However, yellow^{HT} also shows larger displacement factors for Hg. Linear extrapolation of the average displacement parameters perpendicular to the molecular axis (U_{11} and U_{perp}) of yellow^{M} from 293 K to 412 K gives 0.145 and 0.097 Å^2 for Hg and I, respectively. These values are comparable to the corresponding isotropic displacement parameters of yellow^{HT}, 0.142 and 0.079 Å^2. We, therefore, conclude that the displacements may well be dominated by thermal contributions in both structures related to a relatively high mobility of Hg in the packing of I, rather than by disorder effects. The molecule is, thus, highly nonrigid. In the red and orange modifications, the displacement parameters of Hg are of the same order of magnitude or larger than those of I [5–7][10].

In the red and orange modifications, I forms a ccp structure with Hg occupying tetrahedral voids. The transformation between these phases appears to involve only displacements of Hg between different voids, and the crystals are not destroyed. The packing of I in the yellow forms is very distorted in comparison with closest-packed structures. Approximately, closest-packed layers with 6-coordinated spheres may be

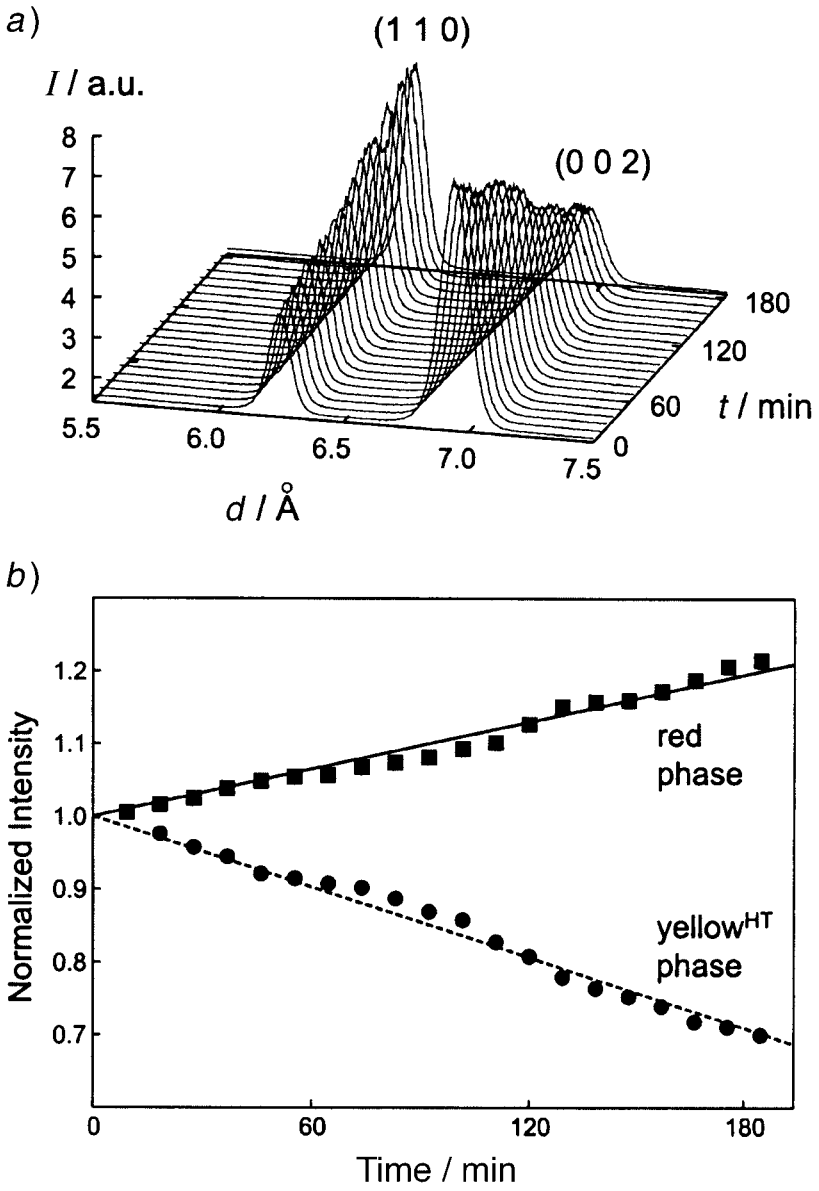

Fig. 8. *Kinetics of the yellow^{HT} → red transition:* a) *raw data collected at 381.3(5) K showing the increase of the (110)$_r$ reflection of the red phase at the expense of the (002)$_y$ reflection of the yellow^{HT} phase*; b) *plot of the integrated intensities, corrected for the decrease of the incoming beam intensity, of these reflections as a function of time.* Intensities normalized to 1.0 at time $t = 0$.

identified that are stacked roughly midway between ccp and hcp. This means that the I substructure is also similar to the cubic volume-centered bcc structure. The transition from yellow to red demands a rearrangement of I and is, therefore, reconstructive.

Upon heating, the transformation appears to proceed by sublimation of the red material in the form of molecules, and yellow nuclei form on the surface [8]. The transformation is destructive: a red single crystal transforms into a yellow^{HT} polycrystal. Our *in situ* high-temperature diffraction studies show that the powder pattern of yellow^{HT} is much more grainy and textured than that of the red starting material, indicating that the newly formed yellow^{HT} crystallites are much larger than the original red ones. This is confirmed by visual inspection at the end of the diffraction experiment. In contrast, upon cooling, the transition may proceed by diffusion of Hg into tetrahedral surroundings in the bulk and subsequent rearrangement of I. This results in a large number of structural defects as evidenced by the intense luminescence of the resulting red crystals.

The solution of HgI_2 in 2-chloroethanol contains molecules, as shown by *Raman* spectroscopy. The yellow^{M} crystals, thus, also grow by accretion of molecules. Even though this is the least-stable form, it is kinetically favored, in agreement with *Ostwald*'s rule [18]: 'In all processes, it is not the most-stable state with the lowest amount of free energy that is initially formed, but the least-stable state lying nearest the free energy of the original state.' The observed dependence of the crystallization from solution on the temperature and on the speed of evaporation affords direct control over which HgI_2 polymorph is predominantly obtained.

We thank Dr. *Jan Helbing* and Prof. *Majed Chergui* for the help with the SHG and luminescence experiments and Dr. *Kurt Schenk* for assistance with the optical microscopy. We also thank the staff of the *Swiss-Norwegian Beam Line* at *ESRF*, Grenoble, for their competent help. This work, as well as the *Swiss-Norwegian Beam/Line*, have been funded by the *Swiss National Science Foundation*. *H. B.* thanks the *Danish Research Training Council* for additional financial support.

Experimental Part

General. Commercial red HgI_2 powder (*Fluka 83379*) was used as acquired and dissolved in 2-chloroethanol. Optical observations were carried out with a *Leitz-SM-POL* microscope equipped with a heating stage to control the temp. of the soln.

Raman *Spectra*. *Raman-SPEX* spectrometer equipped with an Ar laser, 514.5-nm wavelength; recording in a window of 100 to 4000 cm^{-1}, with a typical sampling of 2 cm^{-1} and accumulation time of 1 s. The sat. solns. were contained in capillaries of 0.3 mm diameter.

Second-Harmonic Generation (SHG). An experimental setup for SHG with powders has been reported by *Kurtz* and *Perry* [19]. We performed a similar experiment using a Ti:sapphire laser with wavelength 800 nm and capillaries filled with red HgI_2 powder. Second-harmonic and luminescence signals were measured with a *CCD* detector positioned in backward geometry. A blue filter was placed between the sample and the detector to reduce the background in the second-harmonic measurements. The temp. was controlled with a hot-air blower and was measured with a thermocouple fixed below the capillary. The temp. was corrected for the extra heat from the laser by calibration to the red-to-yellow color change at the known transition temp. of 400(1) K. The laser was kept unfocussed to avoid burning the sample.

Single-Crystal X-Ray Diffraction. The diffraction of the mechanically very unstable yellow^{M} polymorph was carried out with crystals grown on 50-μm *Kapton*® foils. The foil around a crystal suitable for X-ray diffraction was cut and mounted on a glass fiber. Data were collected at r. t. with a *Stoe-IPDS* imaging-plate diffractometer, Mo$K\alpha$ radiation (λ 0.71073 Å) and 2° oscillation range per image. The crystal started to transform into the red form after 60 images. The data were integrated and corrected for *Lorentz* and polarization effects. An anal. absorption correction based on the shape of the crystal was applied. The resulting incomplete data set was sufficient for determining the structure. Fractional coordinates and anisotropic displacement parameters were refined with SHELXL97 [20]; yellow^{M} HgI_2, *M*r 454.39, orthorhombic, $Cmc2_1$, $Z = 4$, $a_o = 4.734(1)$, $b_o = 7.408(2)$, $c_o = 13.943(3)$ Å, $\mu = 43.9$ mm^{-1}, $D_{calc} = 6.173$ g/cm^3, T_{min} 0.212, T_{max} 0.510, 917 measured reflections,

270 unique, 250 observed reflections with $F_o > 4\sigma(F_o)$, $R_1 = 0.055$, $wR_2 = 0.122$, goodness-of-fit 1.168, *Flack* parameter 0.00(9), residual densities $\rho_{max} = 2.1$ and $\rho_{min} = -1.8$ e/Å^3. The resulting atomic parameters are given in Table 1[3]).

Powder Diffraction. The powder-diffraction data for structure determination of the yellow^{HT} phase and the study of the red-to-yellow^{HT} transition were collected at the *Swiss-Norwegian Beam Line*, *ESRF*, Grenoble, on a *MAR345* detector. Focusing optics were used with λ 0.7519(2) Å. The temp. was controlled with a closed helium furnace with a relative precision of 0.2 K. Capillaries with diameters of 0.3 mm were filled either with pure HgI_2 or with a mixture of 50% HgI_2 and 50% diamond powders. The respective particle sizes were 5–10 and 1 μm. The diamond powder served as a standard to ascertain that the amount of HgI_2 in the beam did not decrease appreciably by sublimation; it furthermore reduced the absorption of the sample. The measurement strategy was as follows. The sample-to-detector distance was 190 mm. The receiving slits in front of the sample, which determine the beam size on the sample, were set to 0.4×0.4 mm^2. The detector was operated with 100 μm effective pixel size, which is the highest possible resolution of the *MAR345*. The temp. was slowly raised, and diffraction pictures were recorded every 4 min. by using 60 s exposure time for most images and 360 s for a few. The sample was oscillated during the exposure to improve powder averaging, by 60° for the 60 s and by 359.9° for the 360 s exposures. When the first powder line $(002)_y$ of the yellow^{HT} phase was observed at 402.9(5) K, the temp. was held constant, and the growth of the yellow^{HT} phase was studied with successive exposures during *ca.* 1 h. The temp. was then raised to 404.0(5) K and the subsequent growth was recorded in the same way. After the transformation was complete, diffraction pictures of the yellow^{HT} phase were recorded at 412(2) K for structure determination, with exposure time 30 min, oscillation range 359.9° and sample-to-detector distance 190 mm. The yellow$^{HT} \rightarrow$ red transition was then studied at the constant temp. of 381.3(5) K. The growth of the red phase was monitored with the $(110)_r$ reflection as a function of time during more than 3 h. Finally, the heating system was switched off, and the coexistence of the two phases was observed at a temp. as low as r. t.

The powder-diffraction rings were processed and converted into conventional powder diagrams with the program Fit2D [21]. The diagram recorded at T 412(2) K looks similar to the simulated diagram of the yellow^M polymorph but shows additional weak reflections that cannot be indexed with the orthorhombic unit cell of the yellow^M phase, but instead with the closely related monoclinic cell $\boldsymbol{a}_m = 1.5\,\boldsymbol{a}_o + 0.5\,\boldsymbol{b}_o$, $\boldsymbol{b}_m = -\boldsymbol{c}_o$, $\boldsymbol{c}_m = -0.5\,\boldsymbol{a}_o + 0.5^a\boldsymbol{b}_o$. The systematic absences are $0k0$: $k = 2n+1$. The second-harmonic signal generated by the yellow^{HT} powder indicates a non-centrosymmetric structure, and the space group is thus $P2_1$. Going from $Cmc2_1$ to $P2_1$, a subgroup of index 4, implies two independent I–Hg–I molecules in general positions. Displacing the atoms randomly in steps of 0.02 Å and simulating the corresponding powder pattern produced a first structural model, which was refined according to the *Rietveld* method with GSAS [22]. The profiles were modelled by pseudo-*Voigt* functions. Atoms of the same species were assigned a common isotropic displacement parameter. In total 24 structural parameters were refined, 18 coordinates, 2 displacement parameters, and 4 cell parameters (*Fig. 6*, *Table 2*): yellow^{HT} HgI_2, M_r 454.39, monoclinic, $P2_1$, $Z = 4$, $a_m = 8.0206(7)$, $b_m = 13.9239(7)$, $c_m = 4.4081(3)$ Å, $\beta_m = 95.062(6)°$, $D_{calc} = 6.155$ g/cm^3, confidence factors $N_{obs} = 1773$, $N_{par} = 24$, $Rp = 0.063$, $RWp = 0.087$, $R(F^2) = 0.158$.

REFERENCES

[1] W. Kleber, H. Raidt, K. O. Leupold, *Kristall und Technik* **1968**, *3*, 65.
[2] R. H. Bube, *Phys. Rev.* **1957**, *106*, 703.
[3] M. Piechotka, *Mater. Sci. Eng.* **1997**, *18*, 1.
[4] M. Schieber, H. Hermon, A. Zuck, A. Vilensky, L. Melekhov, R. Shatunovsky, E. Meerson, H. Saado, *Nucl. Instrum. Methods Phys. Res., Sect. A* **2001**, *58*, 41.
[5] G. A. Jeffrey, M. Vlasse, *Inorg. Chem.* **1967**, *6*, 396.
[6] M. Hostettler, H. Birkedal, D. Schwarzenbach, *Acta Crystallogr., Sect B* **2002**, *58*, 903.
[7] M. Hostettler, D. Schwarzenbach, *Acta Crystallogr., Sect. B* **2002**, *58*, 914.
[8] J. B. Newkirk, *Acta Metal.* **1956**, *4*, 316.
[9] C. Guminski, *J. Phase Equil.* **1997**, *18*, 206.
[10] M. Hostettler, H. Birkedal, D. Schwarzenbach, *Chimia* **2001**, *55*, 541.
[11] M. Hostettler, Ph.D. thesis, Université de Lausanne, 2002, Switzerland.

---

[3]) Further details of the crystal-structure investigation may be obtained from the *Fachinformationszentrum Karlsruhe*, D-76344 Eggenstein-Leopoldshafen, Germany, on quoting the depository number CSD 412988.

[12] Y. Marqueton, F. Abba, E. A. Decamps, M. A. Nusimovici, *C.R. Acad. Sci.* (*Paris*) **1971**, *272*, 1014.
[13] R. J. H. Clark, D. M. Rippon, *J. Chem. Soc., Faraday Trans.* **1973**, *69*, 1496.
[14] M. Hargittai, *Chem. Rev.* **2000**, *100*, 2233.
[15] N. Kuroda, T. Iwabuchi, Y. Nishina, *J. Phys. Soc. Jpn.* **1983**, *52*, 2419.
[16] J. L. Merz, Z. L. Wu, L. van den Berg, W. F. Schnepple, *Nucl. Instrum. Methods* **1983**, *213*, 51.
[17] H.-B. Bürgi, *Faraday Discuss.* **2002**, *122*, 41.
[18] W. Ostwald, *Z. Physik. Chem.* **1897**, *22*, 289.
[19] S. K. Kurtz, T. T. Perry, *J. Appl. Phys.* **1968**, *39*, 3798.
[20] G. M. Sheldrick, 'SHELXL97. Program for the Refinement of Crystal Structures', University of Göttingen, Germany.
[21] A. P. Hammersley, ESRF Internal Report 1998, 'FIT2D V9.129', Reference Manual V3.1
[22] A. C. Larson, R. B. von Dreele, 'GSAS Reference Manual 1994, Los Alamos National Laboratory, Report LAUR 86 – 748.

Received February 7, 2003